Steroids 140 (2018) 92–103

Contents lists available at ScienceDirect

Steroids

journal homepage: www.elsevier.com/locate/steroids

Crystal structures and Hirshfeld surface analyses of the di- and tri-hydrates of (5α,17*E*)-17-hydrazonoandrostan-3-ol: Significant differences in the hydrogen bonding patterns and supramolecular arrangements

Ligia R. Gomes[a,b], John N. Low[c], Alan B. Turner[c,1], Thomas C. Baddeley[c], James L. Wardell[c,d,*]

[a] FP-ENAS-Faculdade de Ciências de Saúde, Escola Superior de Saúde da UFP, Universidade Fernando Pessoa, Rua Carlos da Maia, 296, P-4200-150 Porto, Portugal
[b] REQUIMTE, Departamento de Química e Bioquímica, Faculdade de Ciências da Universidade do Porto, Rua do Campo Alegre, 687, P-4169-007 Porto, Portugal
[c] Department of Chemistry, University of Aberdeen, Meston Walk, Old Aberdeen AB24 3UE, Scotland
[d] Instituto de Tecnologia em Fármacos e Farmanguinhos, Fundação Oswaldo Cruz, 21041-250 Rio de Janeiro, RJ, Brazil

ARTICLE INFO

Keywords:
Hydrogen bonds
Crystal structures
Hirshfeld surface analysis
Hydrazones
Androsterones
Molecular electrostatic potential

ABSTRACT

The crystal structures, Hirshfeld surface analyses and electrostatic potential surfaces of the di- and tri-hydrates of (5α,17*E*)-17-hydrazonoandrostan-3-ol, **3**, namely [**3**·(**H$_2$O**)$_2$] and [**3**·(**H$_2$O**)$_3$], are reported. The trihydrate, isolated from a solution of **3** in moist methanol, recrystallizes in the *orthorhombic* space group, $P2_12_12_1$, while that of the dihydrate, isolated from a 1:1 aqueous methanol solution, recrystallizes in the *monoclinic* space group, $P2_1$. The asymmetric unit of the trihydrate involves one steroid and three water molecules, while that of the dihydrate has two similar but independent steroid molecules and four hydrate molecules. Very similar conformations are found for the steroid molecules in both hydrates. As expected, the different mole ratios of water: steroid have major influences on the structures. In both cases, complex crystal structures are constructed from various classical hydrogen bonds, involving the hydrate molecules and the hydroxy and hydrazonyl moieties of the steroid. In the trihydrate, there are no direct connections between the steroid molecules, instead the water molecules link the steroid molecules, with only weak van der Waals forces between the steroid molecules. There are some direct links between the steroid molecules in the dihydrate, involving O—H(steroid hydroxyl)···O (steroid oxo) hydrogen bonds, in a head to head fashion, and O—H···N(hydrazonyl) hydrogen bonds, in a head to tail fashion. However, the major occurrence throughout the structure is of steroid molecules linked by water molecules.

1. Introduction

The functions of 5α-androstane-3α-ol-17-one, **1**, *epi*-androsterone (3α-androstane-3β-ol-17-one, **2**), their derivatives and related steroids, in both plant and animal domains, have attracted much interest [1–5]. As well as the study of synthetic procedures and biological activities, study of the crystal structures of these compounds has been of interest. Among the crystal structures reported include those of **1** and its hemihydrate, both recently confirmed, and that of **2** [6 and references there in], see Scheme 1.

An area of interest in the crystallographic studies has been the linkage of the steroidal molecules via hydrogen bonds. With a donor group, such as a hydroxyl group, at one end, *e.g.,* on C-3, and an acceptor group such as a carbonyl group at the other end of the steroid molecule, *e.g.,* on C-17 [6–14], or vice versa [15], a strong tendency is to form head-to-tail linked molecular chains utilizing O—H···O hydrogen bonds. A strong preference is to use a hydroxy group on C-3 in the O—H···O hydrogen bonding even in the presence of other hydroxyl groups in the steroid. However, in the absence of a 3-hydroxyl group, other hydroxyl groups can be used in the hydrogen bonding with the C-17 carbonyl [16–19].

In hydrates and other solvates, the solvate molecules can play dominate and varying roles in the crystal packing. Thus in the hemihydrate of 5α-androstane-3β-ol-17-one, **6**, the water molecule acts as a link between the androsterone molecules, forming three strong hydrogen bonds, each to a separate androsterone molecule by acting as a donor to two androsterone molecules and an acceptor to a third [6]. The HO unit on C-3 hydroxyl group in androsterone-3β,5α,6β,17β-tetrol·trihydrate [20] acts as the donor in two hydrogen bonds with water molecules as well as acting as an acceptor in O3—H3···O(hydroxyl)

* Corresponding author.
E-mail address: j.wardell@abdn.ac.uk (J.L. Wardell).
[1] Died: 16th February 2014.

https://doi.org/10.1016/j.steroids.2018.09.010
Received 19 July 2018; Received in revised form 19 September 2018; Accepted 24 September 2018
Available online 29 September 2018
0039-128X/

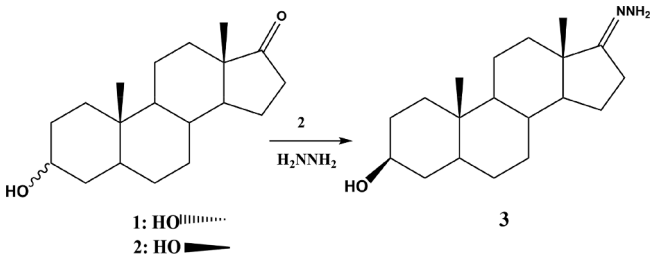

Scheme 1. Formation of **3**.

hydrogen bonds: these link the steroid molecules in a head-to-tail manner. In the methanol solvate of 3β-hydroxyandrost-5-en-17-one, the disordered solvate molecules link pairs of steroid molecules in a head-to-head manner [21]. In contrast, the water molecules in 17α-hydroxy-17-methylandrost-4-ene-3-one·hemi-hydrate [15] appear not to be involved in linking the steroid molecules.

An interesting derivative of 5α-androstane-3β-ol-17-one is the hydrazonylandrostane compound (5α,17*E*)-17-hydrazonoandrostan-3-ol, **3**, prepared from the reaction of *epi*-androsterone, **2** with hydrazine hydrate 80% under reflux [22], see Scheme 1]. Among other things, compound **3** has proved to be a useful precursor of nitrogen containing steroidal heterocycles [23].

Our studies with compound **3** have revealed that hydrates can be obtained on recrystallisation from organic solvents in air. For example slow evaporation of solutions of **3** in moist methanol at room temperature led to the isolation of crystals of a trihydrate, and from a 1:1 (v:v) aqueous MeOH solution, surprisingly only a dihydrate. With hydroxyl and hydrazonyl substituents, in addition to the hydrate molecules, we undertook crystal structure determinations and Hirshfeld surface analyses of these hydrates of **3** to ascertain which of the potential intermolecular interactions were being utilized and how the molecules of **3** are linked.

2. Experimental

2.1. General

Melting points were determined using an MQAPF-302 (MicroQuímica Ltd, Santa Catarina, Brazil) apparatus and are uncorrected. High-resolution mass spectra were determined using a Water Mass Spec. Model Xevo G2 QT of instrument and MassLynx version 4.1 software.

Differential scanning calorimetry. A Mettler Toledo STAR^e System DSC1, cooled by liquid nitrogen and calibrated using indium and zinc as standards, was used with a time–temperature programme of heating from 25 to 250 °C at 10 °C/min.

Thermal gravimetric analysis. A Mettler Toledo STAR^e System TGA2 was used with a time–temperature programme of heating from 25 to 250 °C at 10 °C/min.

2.2. Synthesis

(5α,17*E*)-17-Hydrazonoandrostan-3-ol, **3**, was prepared from the reaction of *epi*-androsterone, **1** with hydrazine hydrate 80% under reflux, as previously reported [22]. The trihydrate and dihydrate were isolated, respectively, from solutions of **3** in moist methanol and 1:1 aqueous methanol and used without further treatment in the structure determinations.

Table 1
Crystallographic experimental details.

	[**3**·(H_2O)$_3$]	[**3**·(H_2O)$_2$]
Crystal data		
Chemical formula	$C_{19}H_{38}N_2O_4$·	$C_{19}H_{36}N_2O_3$
M_r	358.51	340.50
Crystal system, space group	Orthorhombic, $P2_12_12_1$	Monoclinic, $P2_1$
Temperature (K)	200	100
a, *b*, *c* (Å)	5.9299 (2), 12.3916 (4), 28.1777 (9)	7.2600 (2), 9.9010 (2), 26.7004 (6)
α, β, γ (°)	90, 90, 90	90, 94.024 (2), 90
V (Å^3)	2070.52 (12)	1914.53 (8)
Z	4	4
Radiation type	Mo *K*α	Mo *K*α
μ (mm^{-1})	0.08	0.08
Crystal size (mm)	0.30 × 0.27 × 0.20	0.20 × 0.20 × 0.02
Data collection		
Diffractometer	Rigaku AFC12 (Right) diffractometer	XtaLAB AFC12 (RCD3): Kappa single diffractometer
Absorption correction	Multi-scan: *CrysAlis PRO*, Agilent Technologies, Version 1.171.37.35 (release 13-08-2014 CrysAlis171 .NET) (compiled Aug 13, 2014, 18:06:01)	Multi-scan: *CrysAlis PRO* 1.171.39.9g (Rigaku Oxford Diffraction, 2015) Empirical absorption correction using spherical harmonics, implemented in SCALE3 ABSPACK scaling algorithm
T_{min}, T_{max}	0.583, 1.000	0.368, 1.000
No. of measured, independent and observed [$I > 2\sigma(I)$] reflections	15,056, 5210, 4032	24,152, 8680, 8105
R_{int}	0.032	0.033
$(\sin\theta/\lambda)_{max}$ (Å^{-1})	0.695	0.649
Refinement		
$R[F^2 > 2\sigma(F^2)]$, $wR(F^2)$, *S*	0.049, 0.114, 1.02	0.044, 0.101, 1.07
No. of reflections	5210	8680
No. of parameters	264	494
No. of restraints	0	1
H-atom treatment	H atoms treated by a mixture of independent and constrained refinement	H atoms treated by a mixture of independent and constrained refinement
$\Delta\rho_{max}$, $\Delta\rho\sigma_{min}$ (e Å^{-3})	0.15, −0.25	0.33, −0.19
Absolute structure	Flack x determined using 1322 quotients [(I+) − (I−)]/[(I+) + (I−)] [24]	Refined as an inversion twin
Absolute structure parameter	0.3 (5)	0.6 (10)
CCDC deposit numbers	1538473	1817743

Programs used: *CrystalClear*-SM Expert 3.1 b27 [25], *CrysAlis PRO*, Agilent Technologies, Version CrysAlis PRO 1.171.39.9g [26], *CrysAlis PRO*, Agilent Technologies, Version 1.171.37.35, ORTEP [28], SHELXT [29], SHelXle [30], SHELXL7 [31], MERCURY [32], PLATON [33].

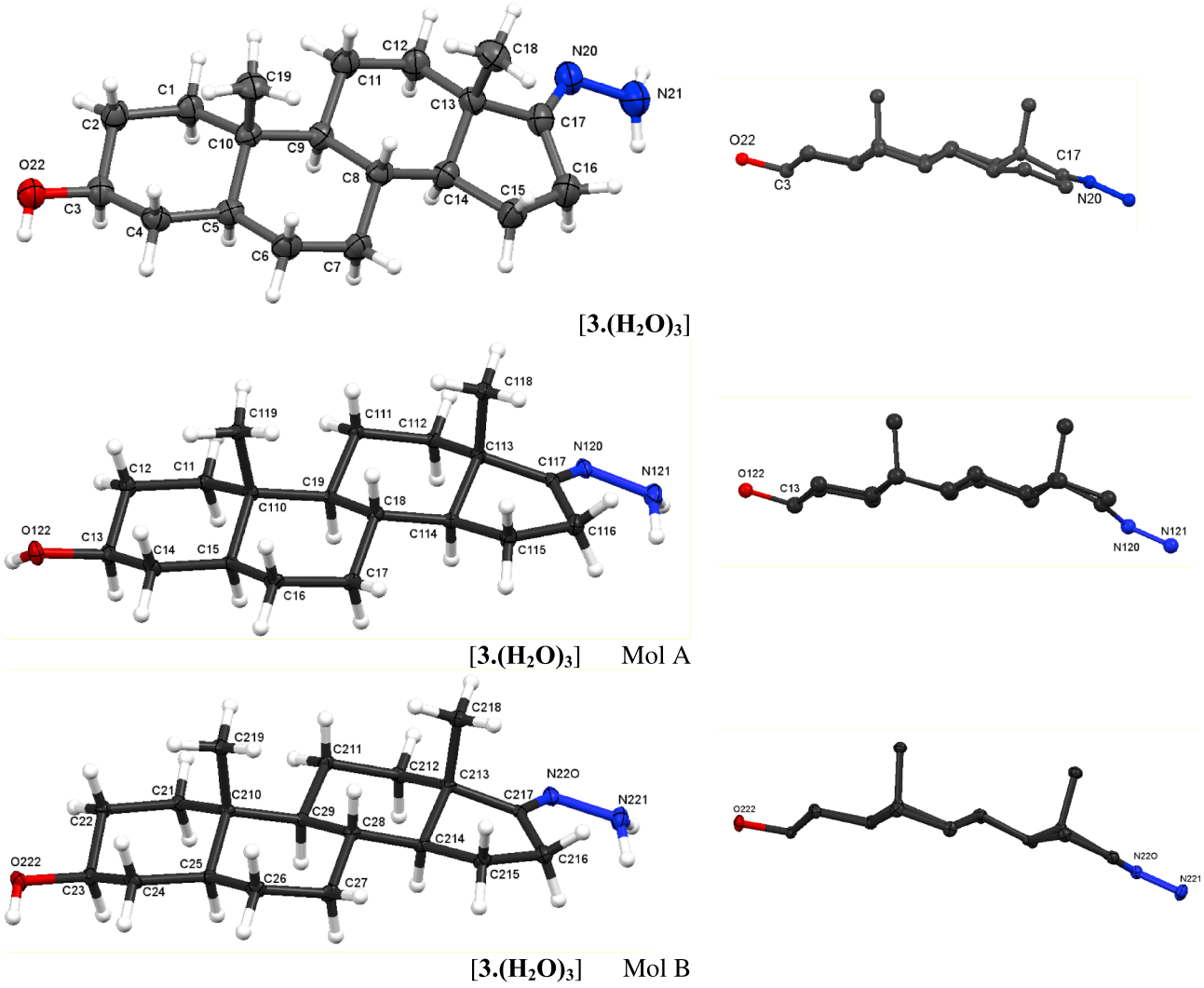

Fig. 1. Atom arrangements and the numbering scheme and side-on views of the molecular conformations of **3** in the two hydrates: ellipsoid probabilities are drawn at the 50% level. Hydrogen atoms have been drawn as spheres of arbitrary radius. Hydrogen atoms have been omitted in the drawings of the conformations.

Table 2
Pucker parameters.

Compound	Q(2), Å	Phi (2), °
Ring D: 5-membered ring		
[**3**·(H_2O)$_3$]	0.460(2)	336.5(3)
[**3**·(H_2O)$_2$]·Mol. A	0.460(2)	203.5(3)
[**3**·(H_2O)$_2$]·Mol. B	0.435(2)	208.5(3)

	Q	Theta	Phi
Six membered rings			
[**3**·(H_2O)$_3$]			
A-ring	0.577(2)	0.4(2)	258(7)
B-ring	0.570(2)	3.0(2)	349(3)
C-ring	0.567(2)	5.9(2)	292(2)
[**3**·(H_2O)$_2$]·Mol. A			
A-ring	0.570(2)	3.3(2)	298(4)
B-ring	0.573(2)	3.9(2)	297(3)
C-ring	0.578(2)	0.0(2)	213(10)
[**3**·(H_2O)$_2$]·Mol. B			
A-ring	0.580(2)	4.4(2)	136(3)
B-ring	0.584(2)	6.9(2)	313.2(19)
C-ring	0.579(2)	3.1(2)	267(3)

Table 3
Geometric parameters and symmetry operations for hydrogen bonds (Å, °).

	D—H···A	D—H	H···A	D···A	D—H···A	Symmetry code
[**3**·(**H$_2$O**)$_3$]	O1W—H1W1···O22^{i}	0.88(4)	1.97(4)	2.851(3)	177(3)	3/2 − x, −y, 1/2 + z
[**3**·(**H$_2$O**)$_3$]	O1W—H2W1···O3W^{ii}	0.92(3)	1.85(4)	2.760(3)	172(3)	−1/2 + x, −1/2 − y, 1 − z
[**3**·(**H$_2$O**)$_3$]	O2W—H1W2···N20^{iii}	0.89(4)	1.93(4)	2.809(3)	172(3)	2 − x, −1/2 + y, 1/2 − z
[**3**·(**H$_2$O**)$_3$]	O2W—H2W2···N21^{iv}	0.85(4)	2.08(4)	2.903(4)	166(3)	3/2 − x, −y, −1/2 + z
[**3**·(**H$_2$O**)$_3$]	O3W—H1W3···O22^{v}	0.83(4)	1.97(4)	2.801(3)	178(5)	5/2 − x, −y, 1/2 + z
[**3**·(**H$_2$O**)$_3$]	O3W—H2W3···O1W	1.00(4)	1.73(4)	2.733(3)	176(4)	
[**3**·(**H$_2$O**)$_3$]	N21—H21B···O3W	0.89(4)	2.15(4)	2.995(3)	159(3)	
[**3**·(**H$_2$O**)$_3$]	O22—H22···O2W	0.79(4)	1.89(4)	2.677(3)	174(3)	
[**3**·(**H$_2$O**)$_2$]	O3—H3X···N120	0.83(3)	2.18(3)	2.988(3)	164(3)	1 − x, −1/2 + y, 1 − z
[**3**·(**H$_2$O**)$_2$]	O3—H3Y···O122	0.88(5)	2.11(5)	2.963(3)	165(4)	
[**3**·(**H$_2$O**)$_2$]	O4—H4X···N220	0.87(4)	2.04(4)	2.903(3)	169(3)	1 − x, 1/2 + y, −z
[**3**·(**H$_2$O**)$_2$]	O4—H4Y···N121	0.89(4)	2.00(3)	2.873(3)	170(3)	1 − x, 1/2 + y, 1 − z
[**3**·(**H$_2$O**)$_2$]	O5—H5X···O222	0.78(5)	2.13(5)	2.904(3)	171(4)	−1 + x, y, z
[**3**·(**H$_2$O**)$_2$]	O5—H5Y···O4	0.90(4)	1.96(4)	2.826(3)	161(3)	
[**3**·(**H$_2$O**)$_2$]	O6—H6X···N220	0.86(5)	2.60(4)	3.243(3)	133(3)	1 − x, 1/2 + y, −z
[**3**·(**H$_2$O**)$_2$]	O6—H6Y···O5	0.86(4)	1.91(4)	2.751(4)	178(5)	
[**3**·(**H$_2$O**)$_2$]	O122—H122···O6	0.86(4)	1.77(4)	2.626(3)	176(3)	
[**3**·(**H$_2$O**)$_2$]	N121—H124···O222	0.87(4)	2.24(4)	3.011(3)	149(3)	2 − x, 1/2 + y, 1 − z
[**3**·(**H$_2$O**)$_2$]	O222—H222···O122	0.82(3)	1.90(3)	2.724(2)	175(3)	
[**3**·(**H$_2$O**)$_2$]	N221—H224···O3	0.89(4)	2.19(3)	3.050(3)	164(3)	1 − x, 1/2 + y, −z

Table 4
Percentages of the most important atom–atom contacts involving **3**.

	H···H	H···O	O···H	H···N	N···H	H···C/C···H
[**3**·(**H$_2$O**)$_3$]	85.4	6.6	2.9	0.8	4.1	0.2
[**3**·(**H$_2$O**)$_2$]·Mol. A	84.8	6.9	2.8	0.6	4.7	0.1
[**3**·(**H$_2$O**)$_2$]·Mol. B	85.2	5.3	3.4	0.8	4.8	0.4

2.3. Compound [3·(H$_2$O)$_3$]

M.p. 187–192 °C.

HR-MS (ESI): Calcd for $C_{19}H_{33}N_2O^+$ (**3** + H^+): 305.2587; Found: 305.2596.

2.4. Compound [3·(H$_2$O)$_2$]

M.p. 195–199 °C.

HR-MS (ESI): Calcd. $C_{19}H_{33}N_2O^+$ (**3** + H^+): 305.2587; Found: 305.2590.

2.5. Experimental crystallography

All details are listed in Table 1 [24–33].

2.6. Hirshfeld surface analyses

The Hirshfeld surfaces and two-dimensional Fingerprint (FP) plots [34] were generated using Crystal Explorer 3.1 [35]. The Hirshfeld surface mapped over d_{norm} was scaled between −0.750 and 1.560. The electrostatic potential (ESP) was calculated with TONTO [36] as implemented in Crystal Explorer 3. The surfaces computed refer only to the steroid part of the compound. The same applies to the percentages of the various contacts, which were selected by the partial analysis of the FP plots.

3. Results and discussion

Crystals of the trihydrate of **3** were isolated by slow evaporation of a solution of **3** in moist methanol maintained at room temperature, over 5 days while those for the dihydrate were harvested after 3 days from a 1:1(v:v) aqueous methanol solution maintained at room temperature in air.

The asymmetric unit of [(**3**)·(**H$_2$O**)$_3$] consists of a single molecule of **3** and three water molecules, while that of [(**3**)·(**H$_2$O**)$_2$] consists of two independent molecules, Mol. A & Mol. B, of **3** and four water molecules. The trihydrate, [**3**·(**H$_2$O**)$_3$], recrystallises in the *orthorhombic* space group, $P2_12_12_1$ and the dihydrate in the *monoclinic* space group, $P2_1$. The atom arrangements, numbering schemes and molecular conformations of the steroidal molecules in both hydrates are shown in Fig. 1.

The three six-membered rings in each molecule of **3** in both hydrates have ideal or near ideal chair shapes, while the five membered rings in [(**3**)·(**H$_2$O**)$_3$] and Mol. B of [(**3**)·(**H$_2$O**)$_2$] have envelope shapes with the flaps at C14 and C24, respectively, and that of Mol. A of [(**3**)·(**H$_2$O**)$_2$] has a twist on C113—C114, see Table 2. Thus there are only minor differences between the conformations of molecules of **3** in both hydrates. The bond lengths and angles are all in the expected regions and are not further discussed.

3.1. Intermolecular interactions

A large number of classical hydrogen bonds in both hydrates, as determined using PLATON [33], and confirmed by the Hirshfeld surface analyses [34,35], link the steroid and the water molecules into complex three-dimensional arrays, see Table 3 for the intermolecular interactions and symmetry operations. As a consequence of the steroid nature of the molecule, the most abundant contacts involving the steroid molecules are H···H contacts, see Table 4. Table 4 lists the contact percentages, selected by partial analyses of the FP plots. As well as the hydrate molecules, the two functional groups, H_2N—N and HO, at opposite ends of the steroid molecule, **3**, are involved in classical hydrogen bonds. These result in the N/O—H···O interactions listed in Table 3. Only small percentages of H···C/C···H are noted. As shown in Table 3 there are only small differences in the percentages of contacts involving the steroid molecules.

3.1.1. Supramolecular arrangements in [(3)·(H$_2$O)$_3$]

As indicated in Table 3, each hydrate molecule is involved as a donor in two hydrogen bonds and as acceptor in another. Both nitrogen atoms of the hydrazonyl group also act as acceptor atoms, but only one of the hydrogens in each =N-NH_2 moiety is utilized in hydrogen bonding in [(**3**)·(**H$_2$O**)$_3$]. Each of the three independent water molecules is involved in different sets of hydrogen bonds, see Table 3. Thus (i) water molecule, W*1 (with O1W), acts a donor to a HO group of a steroid molecule, and as an acceptor and a donor in two hydrogen bonds with two molecules of W*3, (ii) W*2 (with O2W), acts as donor

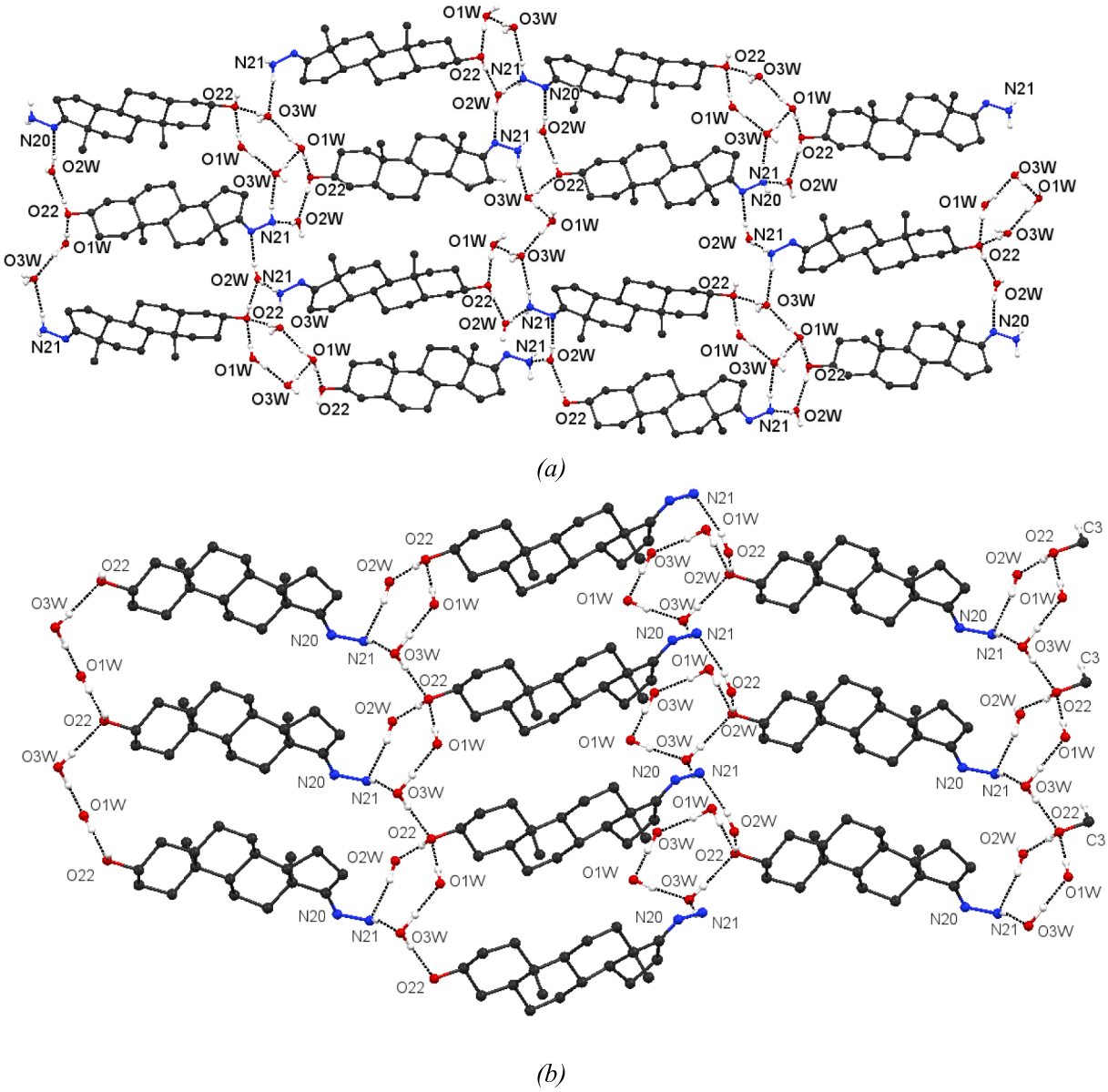

Fig. 2. [**3**·(**H$_2$O**)$_3$]. (a) Part of a slice through the 3-dimensional structure showing a puckered sheet of molecules, viewed down the *a* axis, (b) part of another slice through the three dimensional hydrogen-bonded structure, this time looking down the *b* axis: this slice shows a regular stacking arrangement of the steroid molecules. The various hydrogen bonds are drawn as thin dashed lines. Symmetry operations are listed in Table 2.

to two molecules of **3**, via the N20 and N21 atoms, and as an acceptor to the HO group of a steroid molecule, and (iii) water molecule, W*3 (with O3W) acts as a donor to the HO group of a steroid molecule and to W*1, and as acceptor to another W*1 and to the HN moiety of another steroid molecule. The hydroxyl group of the steroid acts as an acceptor to both W*1 and W*3 and a donor to W*2, while the =N-NH$_2$ moiety acts as acceptor to two W*2 and as a donor to W*3 molecules. There are no direct steroid to steroid links.

Involvement of all the hydrogen bonds results in a overall complex three-dimensional structure. Different slices through the three dimensional hydrogen bonded structure reveal different molecular arrangements generated from different combinations of hydrogen bond. Examples of such slices are illustrated in Fig. 2. It is also apparent that spiral chains of molecules, formed from hydrogen bonds, occur throughout the structure. As can be observed in the two slices shown in Fig. 2, different combinations of hydrogen bonds, generated from the water molecules and the HO and H$_2$N-N= moieties of molecule **3**, create different complex chains within the slices, which effectively segregate the steroid molecules within columns. These hydrogen bonded chains are further linked into a more elaborate hydrogen bonded framework throughout the structure as shown in Fig. 3: only the atoms in 3 which participate in the hydrogen bonding network have been drawn for reasons of clarity. The arrangement shown in Fig. 3 contains a network of various rings, including $R_5^5(10)$, $R_5^5(12)$, and $R_6^6(14)$ rings [37].

Three views of the Hirshfeld surface of the steroid molecule in [**3**·(**H$_2$O**)$_3$] are illustrated in Fig. 4, which also show the connections of **3** with the three water molecules W*1, W*2 and W*3. The red areas indicate contact points at the hydroxyl and =NNH$_2$ groups of the steroid, which result from O3W—H1W3···O22, O1W—H1W1···O22, and

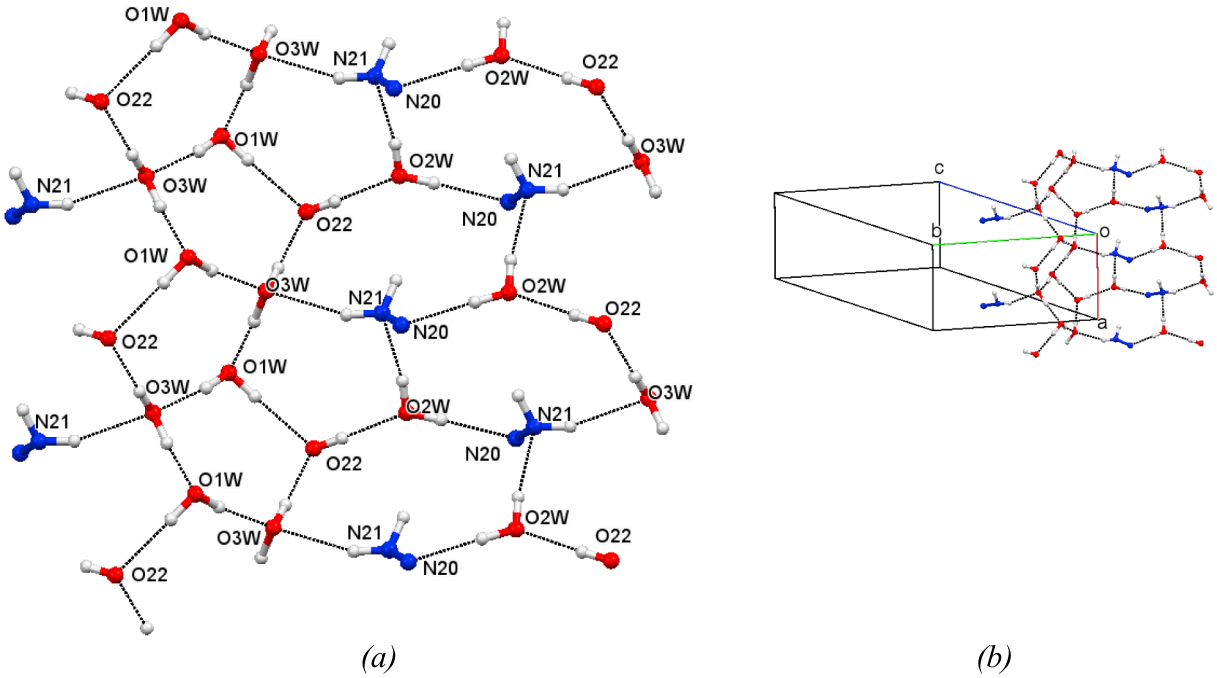

Fig. 3. [**3**·($\mathbf{H_2O}$)$_3$]. (a) Part of the hydrogen bond framework, formed from the water molecules, and the HO and H_2N-N═ moieties of molecule **3**. Only the participating atoms of **3** in the hydrogen bonding network are drawn, (b) another view of the hydrogen bonded network showing the cell axes. As can be seen, each of the three independent water molecules are involved in different sets of hydrogen bonds, see also Table 2.

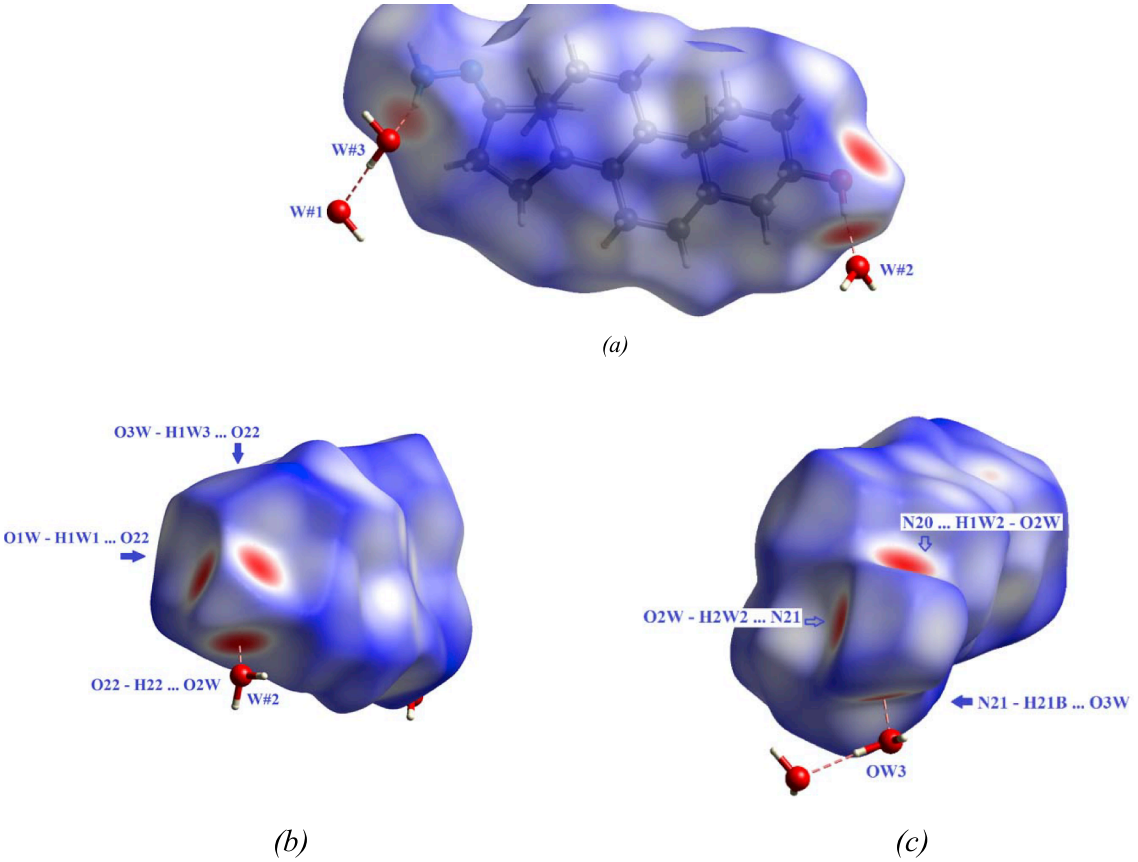

Fig. 4. Three views of the Hirshfeld surface of **3** in [**3**·($\mathbf{H_2O}$)$_3$], mapped over d_{norm}, (a) Connections of **3** with W*2, via O22, and with W*3, via ═NNH_2, also showing is a further link to W*1, (b) the highlighted red spots indicate contact points with the hydroxyl atoms of the steroid, due to O3W—H1W3···O22, O1W—H1W1···O22, and O22—H22···O2W hydrogen bonds, (c) the three highlighted red spots indicate contact points with the ═NNH_2 atoms of the steroid, (N21—H21B···O3W, N21···H2W2—O2W and N20···H1W2—O2W, as designated, also a small red spot area on the top face has a complementary spot on the hidden face and is due to a C···H contact.

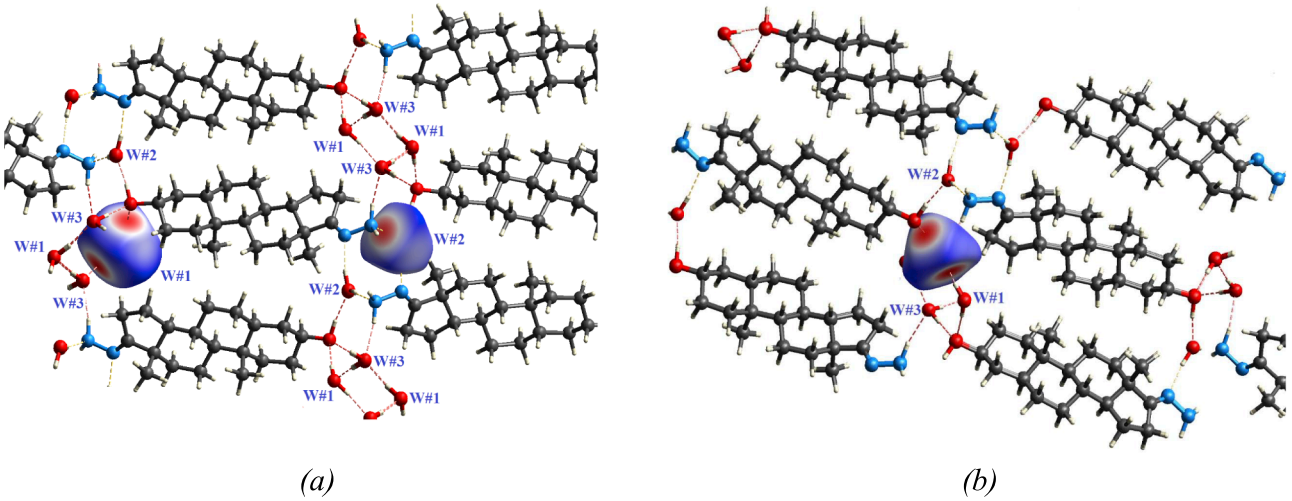

Fig. 5. Views of the Hirshfeld surfaces mapped over d_{norm} of the three water molecules, W#1, W#2 and W#3, in [**3**·($\mathbf{H_2O}$)$_3$]: also indicated are their immediate connections. The highlighted red spots on the surfaces indicate contact points with the N/O···H atoms (dashed lines: red for O···H and yellow for N···H). The positions of additional water molecules W#1, W#2 and W#3 with contacts to the identified hydrate molecules are also indicated.

O22—H22···O2W, N21—H21B···O3W, N21···H2W2—O2W and N20···H1W2—O2W hydrogen bonds. There is also a small red area on the top face, with a complementary spot on the hidden face, these arise from C···H contacts. Fig. 5 illustrates the Hirshfeld surfaces of the three hydrate molecules. The immediate connections to the water molecules are also highlighted as are the red areas indicating contact points with N/O···H atoms.

3.1.2. *Supramolecular arrangements in [(**3**)·($\mathbf{H_2O}$)$_2$]*

A consequence of having two steroid molecules and four water molecules in the asymmetric unit of the dihydrate is that a larger number of classical hydrogen bonds have to be considered than those involved in the trihydrate, with just one steroid and three hydrate molecules in the asymmetric unit. The different steroid to hydrate mol ratio results in significant differences in the supramolecular arrays of the two hydrates. With a reduction in the relative amount of water molecules, there are now some direct links between the steroidal molecules in the dihydrate: molecules, A and B, are directly linked by N121—H124···O222 and O222—H222···O122 hydrogen bonds. Of interest, these direct links involve hydroxyl–hydroxy and hydrazonyl–hydroxy interactions but not hydrazonyl–hydrazonyl interactions.

Both hydrogen atoms and the oxygen atom of each hydrate molecule, termed W*3 to W*6, are involved in the hydrogen bonding scheme in the trihydrate, see Table 2. However it is noticeable that the proportion of nitrogen to oxygen atoms involved as acceptors towards the hydrate molecules changes from 2:4 in the trihydrate to 5:4 in the dihydrate. These changes are still significantly different to the ratios of nitrogen to oxygen atoms in the trihydrate and dihydrate of 2:4 and 4:6, respectively. Both nitrogen atoms of each hydrazonyl group in [(**3**)·($\mathbf{H_2O}$)$_2$] act as acceptor atoms, but only one of the hydrogens in each =N-NH$_2$ moiety is utilized in hydrogen bonding in [(**3**)·($\mathbf{H_2O}$)$_2$]. The steroidal hydroxyl groups in Mol. A (with O122) and Mol. B (with O222) are involved in different sets of hydrogen bonds, thus the OH group in Mol. A acts as an acceptor to both W*3 and the hydroxyl group of Mol. B, and as a donor to W*6, while the OH group of Mol. B acts as an acceptor to W*5 and to the =N-NH$_2$ unit of Mol. A and as a donor to the hydroxyl group of Mol. A.

The combination of all the intermolecular interactions generates a complex three dimensional supramolecular array. As in the trihydrate, different slices through the three dimensional structure of the dihydrate reveal different molecular arrangements formed from different combinations of hydrogen bonds. Two such slices are illustrated in Fig. 6. In each of these slices, complex chains, formed from the combinations of hydrogen bonds, effectively separate the steroid molecules into columns. It is also apparent that spiral chains of molecules, linked by hydrogen bonds, occur throughout the structure. These complex hydrogen bonded chains, observed in the slices, are further linked into a more elaborate hydrogen bonded framework throughout the structure as shown in Fig. 7: only the atoms in **3** which participate in the hydrogen bonding network have been drawn for reasons of clarity. Each of the four independent water molecules is involved in different sets of hydrogen bonds, see Table 2 and Fig. 8. Thus, (i) water molecule, W*3, is hydrogen bonded to a Mol. B of **3**, via its H$_2$N-N= group, a Mol. A of **3**, via its OH group and to W*4, (ii) water molecule W* 4, to the H$_2$N-N= groups of both Mol. A and Mol. B and to W*5, (iii) water molecule, W*5, to HO of Mol. B, W*6 and W*4, and (iv) and water molecule, W*6, to HO of Mol. A, H$_2$N-N= group of Mol. B and to W*5. The network shown in Fig. 7 contains a set of $R_5^5(10)$, $R_5^5(12)$, and $R_6^6(14)$ rings [37].

Views of the Hirshfeld surfaces for both Mol. A and Mol. B are illustrated in Fig. 8, which also indicates the direct contacts between the steroid molecules, O222—H222···O122, and N121—H124···O222, and connections to the four water molecules, W*3–W*6, i.e., O3—H3Y···O122, O3—H3X···N120, N221—H224···O3, O4—H4X···N220, O4—H4Y···N121, O5—H5X···O222, O122—H122···O6 and O6—H6X···N221. There is also a small red area on the top face, which has a complementary spot on the hidden face and is due to a C···H contact. Fig. 9 illustrates the Hirshfeld surfaces of the four hydrate molecules. The immediate connections to other water molecules are also highlighted as are the contact points with the N/O···H atoms. The FP plots for both hydrates are shown in Fig. 10.

3.2. *Molecular electrostatic potential (ESP)*

Because Hirshfeld surface partitions of the crystal space give non-overlapping volumes associated with each molecule, these surfaces

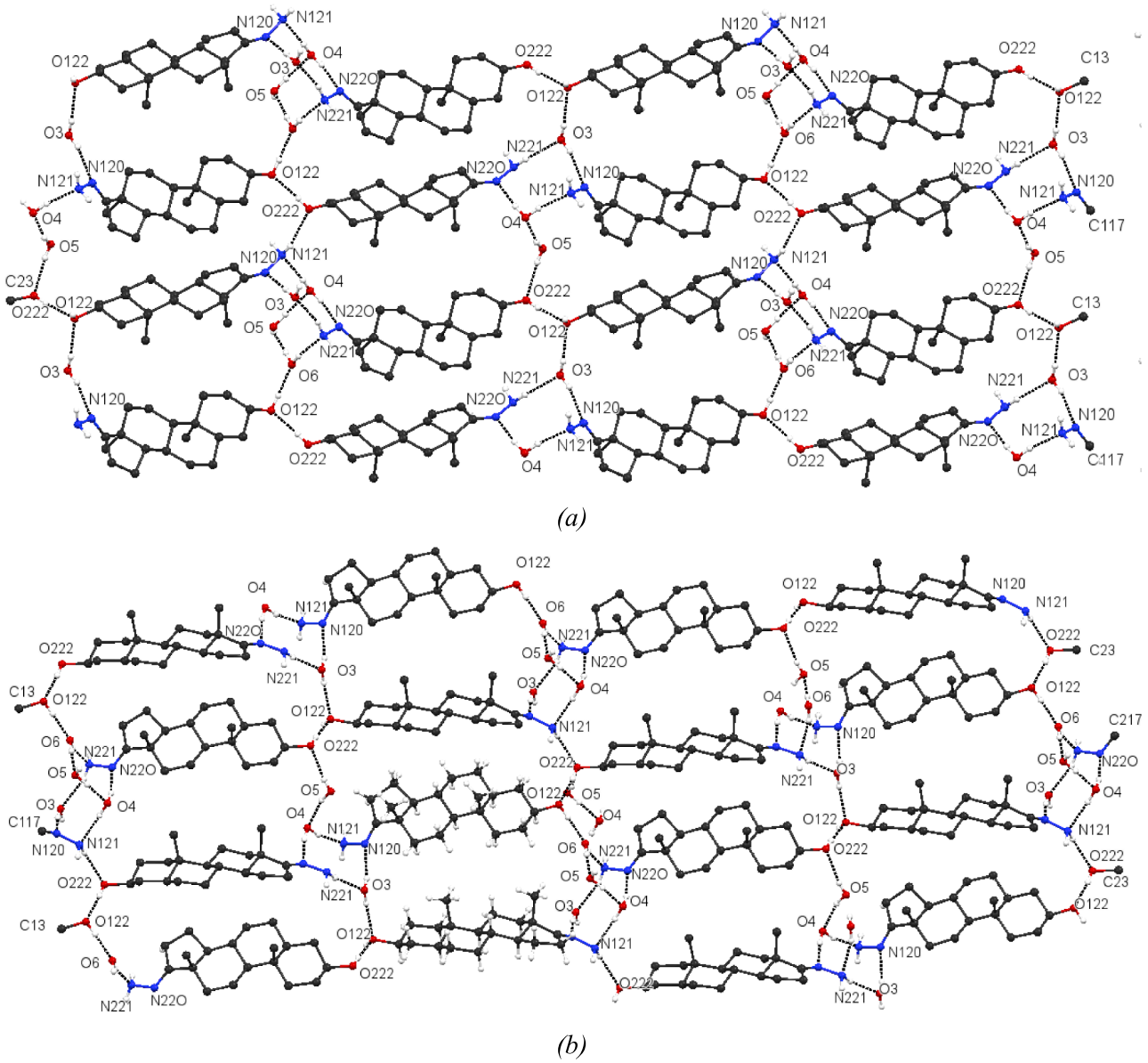

Fig. 6. [**3**·(H_2O)$_2$]. (a) Part of a slice through the 3-dimensional structure showing a puckered sheet of molecules, viewing down the *a* axis, (b) part of another slice through the three dimensional hydrogen-bonded structure, this time looking down the *b* axis. The various hydrogen bonds are drawn as thin dashed lines. Symmetry operations are listed in Table 2.

provide a kind of "electrostatic complementarity". Negative electrostatic potential regions are represented by red areas and those of electropositive domains by blue areas. The grey areas on the remaining mapped Hirshfeld surfaces indicate regions close to electroneutrality. Thus as shown in Fig. 11a and b, for the trihydrate, regions close to the lone pairs on the oxygen atom of the hydroxyl group and the nitrogen atoms of the hydrazonyl group are shown as red areas. The blue regions, the electropositive domains, are located near the H atoms of the hydroxyl and hydrazonyl groups, Fig. 11c. In Fig. 11c, the electrostatic complementarity of the N/O—H···O (water) contacts of the steroid with hydrate molecules is highlighted: here the hydrogen atoms of the hydroxyl and hydrazonyl groups involved in the N/O—H···O (water) contacts are indicated by the blue regions just above the surface of the steroid molecule.

The Hirshfeld surfaces mapped with electrostatic potential of both independent molecules of [**3**·(H_2O)$_2$], are provided in Fig. 12. Fig. 12a illustrates the electropositive area of Mol. B involved in the direct contact [via the hydrogen atom of its hydroxyl group] with the lone pair of the oxygen atom of the −OH group of Mol. A, thereby creating the O222—H222···O122 hydrogen bond. In Fig. 12b is illustrated the other direct contact between Mol. A with Mol. B via the electropositive area of Mol. A [hydrogen atom of its hydroxyl group] with the formation of the N121—H124···O222 hydrogen bond. In Fig. 12c, Hirshfeld surfaces of both molecules of [**3**·(H_2O)$_2$] are shown. The remaining blue

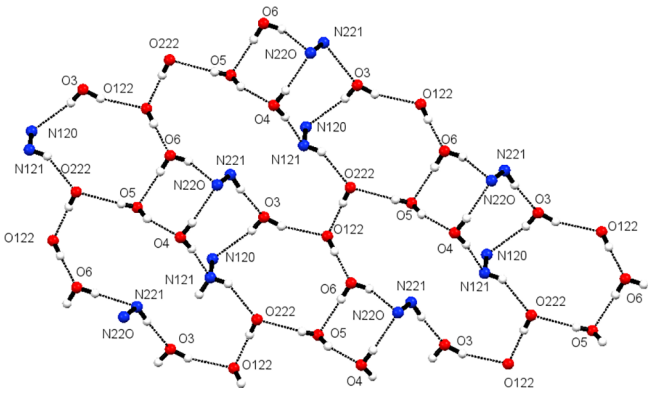

Fig. 7. [**3**·(H_2O)$_2$]. (a) Part of the hydrogen bond framework, formed from the water molecules, and the HO and H_2N-N= moieties of molecule **3**. Only the participating moieties within **3** in the hydrogen bonding network are drawn. Each of the four independent water molecules are involved in different sets of hydrogen bonds, see also Table 2 for symmetry operations. The hydrogen bonds are drawn as thin dashed lines.

and red areas are due to interactions with water molecules.

3.2.1. DSC and TGA studies of [(3)·(H_2O)$_2$]

Differential scanning calorimetry. A Mettler Toledo STAR^e System DSC1, cooled by liquid nitrogen and calibrated using indium and zinc as standards, was used. A sample of the dihydrate, [(**3**)·(H_2O)$_2$] (8.63 mg), was used with a time–temperature program of heating from 25 to 250 °C at 10 °C/min. The DSC trace, see Supplementary Fig. 1, indicates a glass transition occurring at an initial temperature of 101.65 °C with a peak at 115.2 °C, corresponding to an energy of 8.9 kJ/mol. The onset of melting occurred at 195 °C, with the peak at 199 °C; the corresponding energy is 24.2 kJ/mol.

Thermal gravimetric analysis. A Mettler Toledo STAR^e System TGA2 was used. A sample of the dihydrate [(**3**)·(H_2O)$_2$], 15.69 mg, was used with a time–temperature program of heating from 25 to 250 °C at 10 °C/min. Two significant mass loss regions (i) 4.98% mass loss between 39 and 106 °C and (ii) 5.46% between 106 and 146 °C, see Supplementary Fig. 2. The molecular weight of [(**3**)·(H_2O)$_2$] is 340.50, and hence the calculated percentage loss of one hydrate molecule is 5.28%. The combined weight loss is that of the two hydrates [total 10.56%, compared to the found loss of 10.44%]. Thus the dehydration of [(**3**)·(H_2O)$_2$], occurs essentially stage by stage, with just a small overlap.

Successive loss of the three hydrate molecules from the trihydrate, [(**3**)·(H_2O)$_3$], are expected too.

4. Conclusions

The combination of the Hirshfeld pixel approach and the PLATON geometric approach provides complimentary insights into the supramolecular structure of [(**3**)·(H_2O)$_2$] and [(**3**)·(H_2O)$_3$]. Strong classical hydrogen bonds in both hydrates, utilizing the hydrate molecules and the hydroxyl and hydrazono moieties of the steroid, generate different complex three dimensional structures. There are no direct steroid–-steroid contacts in the trihydrate, but there are some head-to-head and head to tail direct contacts in the dihydrate, although hydrate linked steroid–steroid contacts still dominate. The influence of the number of hydrate molecules on the overall structure, in particular on the contact between the steroid molecules, is clearly apparent.

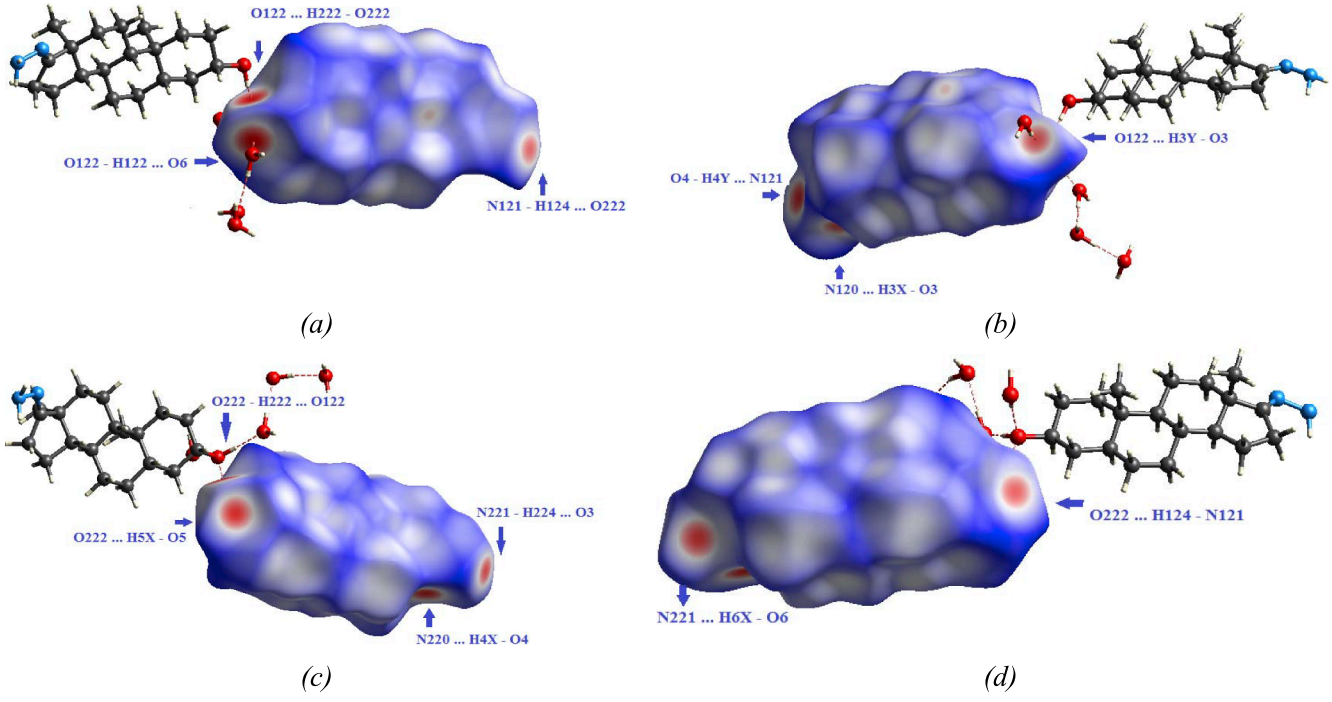

Fig. 8. [**3**·(H_2O)$_2$]. Views of the Hirshfeld surfaces mapped over d_{norm} of (a) and (b) Mol. A, (c) and (d) Mol. B. The highlighted red spots on the surfaces indicate contact points with the O—H and the N-NH_2 atoms of the steroid as identified. The small red area on the top face of c arises from C···H contacts.

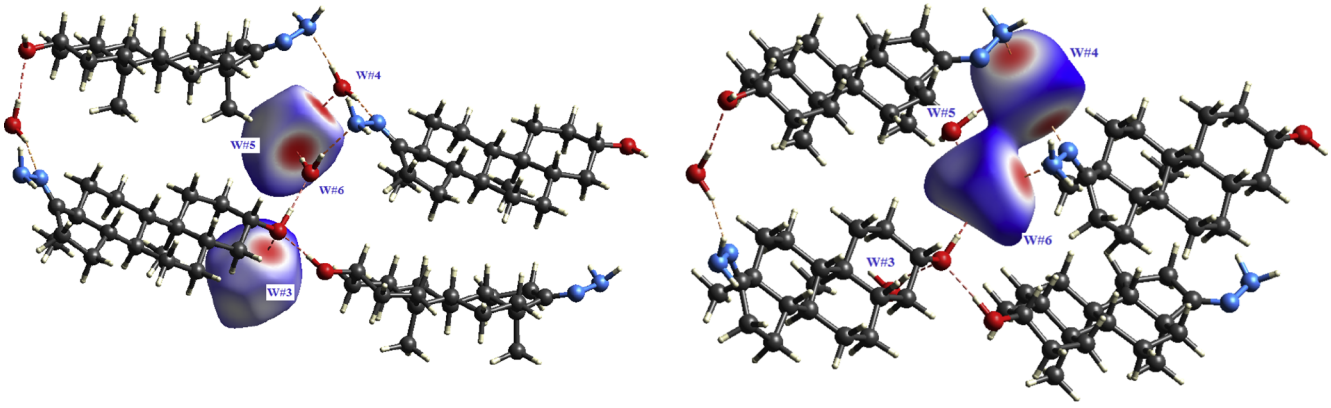

Fig. 9. [**3**·(**H_2O**)$_2$]. Views of the Hirshfeld surface mapped over d_{norm} for the hydrate molecules, W#3, W#4, W#5 and W#6. The highlighted red spots on the surfaces indicate contact points with the N/O···H atoms (dashed lines: red for O···H and yellow for N···H). Contacts with the highlighted water molecules by molecules of **3** and other water molecules are indicated.

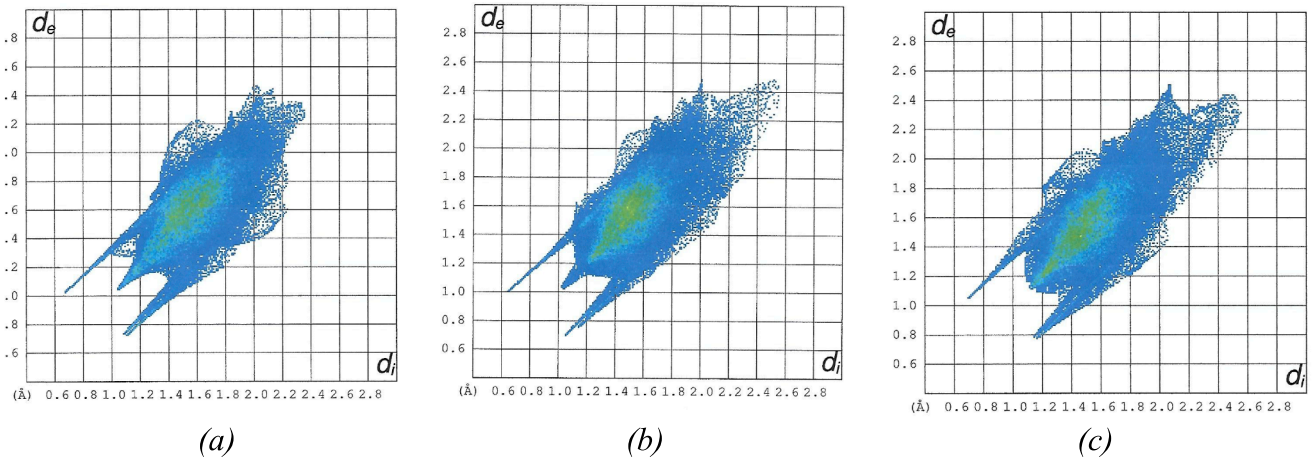

Fig. 10. The FP plots for the molecule **3** in (a) [**3**·(**H_2O**)$_3$], (b) Mol. A of [**3**·(**H_2O**)$_2$] and (c) Mol. B of [**3**·(**H_2O**)$_2$]. The light blue areas in the middle of the FP plots at de/di ≅ 1.6 Å show high pixel frequencies due to H···H contacts. The sharp spikes pointing to southwest are due to N/O···H contacts: the inner ones on the right are due to O···H contacts; the outer ones on the right are related to N···H contacts. The left spikes are due to the H···O contacts.

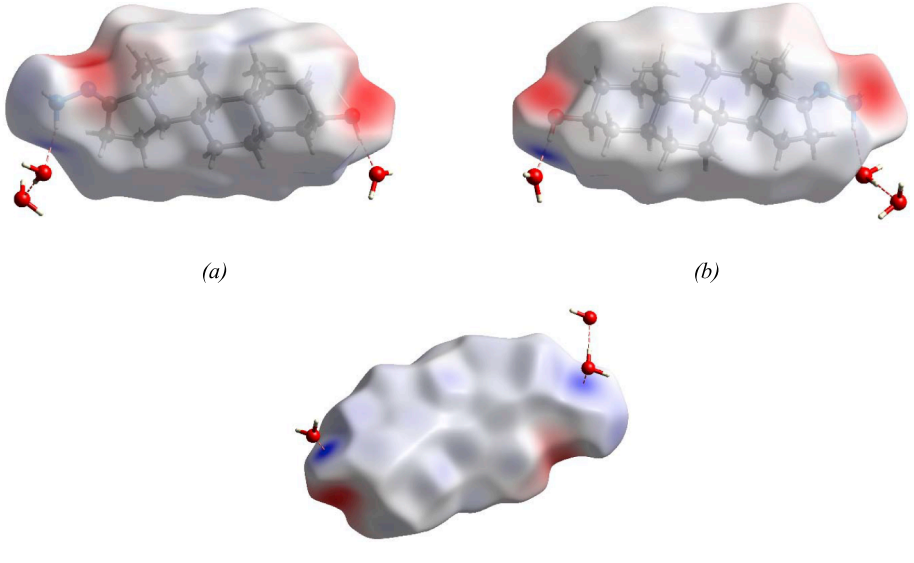

Fig. 11. The electrostatic potential surfaces for molecule **3** in [**3**·(**H_2O**)$_3$]. The surfaces show the complementary electropositive areas (blue) with the water molecules. The ESP (ranging from −0.077 to 0.066) is electronegative in the vicinity of the lone pairs of the oxygen atom and of the lone pairs of the nitrogen atoms of the hydrazide fragment.

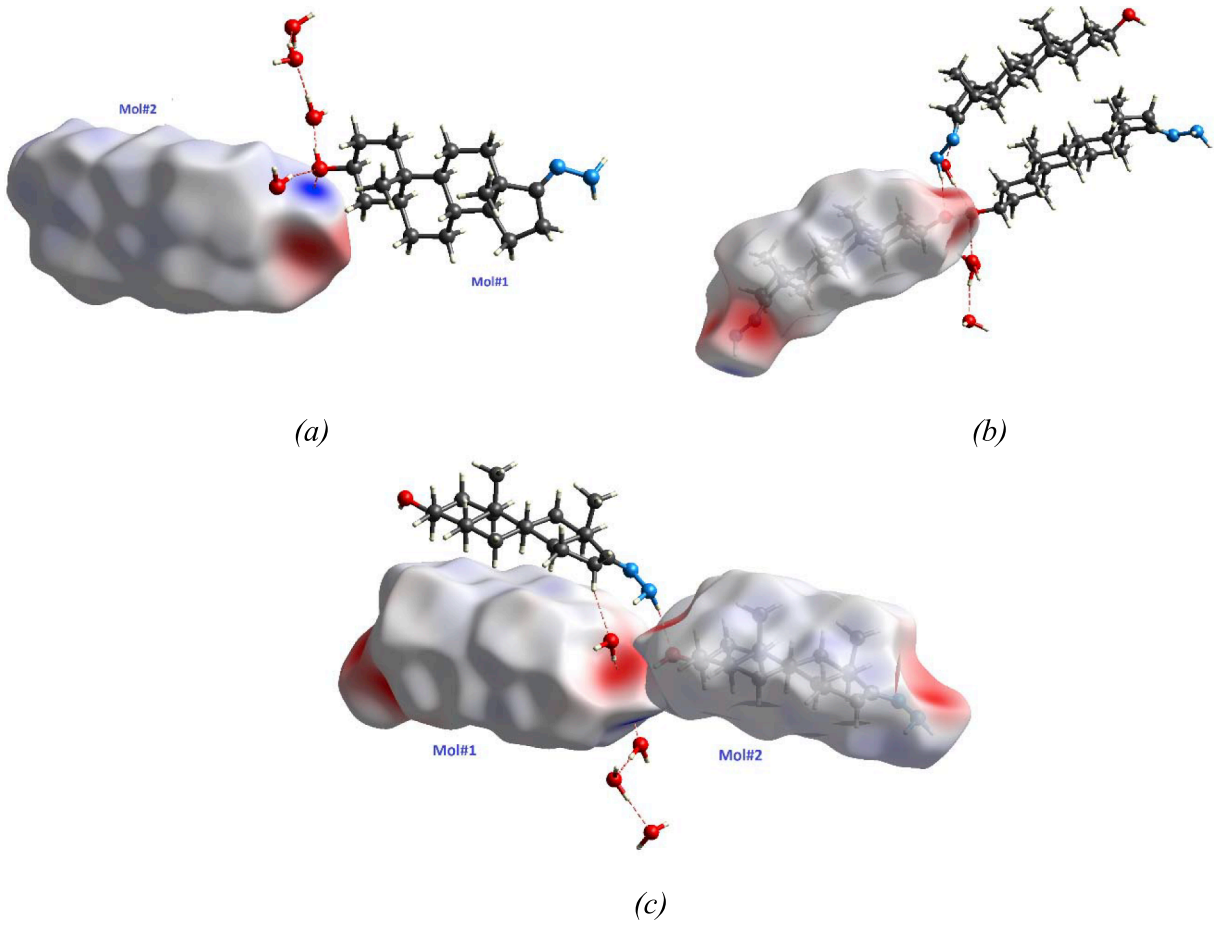

Fig. 12. Hirshfeld surfaces for **3** in [(**3**)·(H_2O)$_2$] **2** mapped with electrostatic potential. (a) The electropositive area of Mol. B indicating the interaction site with the lone pair of the oxygen atom of the HO group of Mol. A, (b) the electronegative area of Mol. B indicating interaction with another steroid involving a NH···O hydrogen bond, (c) Hirshfeld surfaces of Mol. A and Mol. B. The remaining blue and red areas are due to interactions with water molecules.

Acknowledgements

The authors thank the National Crystallographic Service, University of Southampton for the data collection, and for their help and advice. This work was supported by the Portuguese Foundation for Science and Technology (FCT) UID/Multi/04546/2013 and by CNPq, Brazil.

Appendix A. Supplementary data

Supplementary data to this article can be found online at https://doi.org/10.1016/j.steroids.2018.09.010 and have also been deposited with the Cambridge Crystallographic Data Centre with deposition number CCDC 1538473 and 1817743 for [**3**·(H_2O)$_3$] and [**3**·(H_2O)$_2$], respectively. Copies of these can be obtained free of charge on written application to CCDC, 12 Union Road, Cambridge, CB2 1EZ, UK (fax: +44 1223 336033); on request by e-mail to deposit@ccdc.cam.ac.uk or by access to http://www.ccdc.cam.ac.uk.

References

[1] R.A. Prough, B.J. Clark, C.M. Klinge, Novel mechanisms for DHEA action, J. Mol. Endocrin. 56 (2016) R139–R155.
[2] L. El Kihel, Oxidative metabolism of dehydroepiandrosterone (DHEA) and biologically active oxygenated metabolites of DHEA and epiandrosterone (EpiA) – recent reports, Steroids 77 (2011) 10–22.
[3] P. Lindemann, Steroidogenesis in plants – biosynthesis and conversions of progesterone and other pregnane derivatives, Steroids 103 (2015) 145–152 Special Issue.
[4] L. Gauthier-Landry, A. Belanger, O. Barbier, Multiple roles for udp-glucuronosyltransferase (UGT)2B15 and UGT2B17 enzymes in androgen metabolism and prostate cancer evolution, J. Steroid Biochem. Mol. Biol. 145 (2015) 187–192.
[5] A. Robic, T. Faraut, A. Prunier, Pathways and genes involved in steroid hormone metabolism in male pigs: a review and update, J. Steroid Biochem. Mol. Biol. 140 (2014) 44–55.
[6] A.T. Hulme, R.W. Lancaster, H.F. Cannon, Clarification of the crystalline forms of androsterone, CrystEngComm 8 (2006) 309–312.
[7] C.M. Weeks, A. Cooper, D.A. Norton, H. Hauptman, J. Fisher, The crystal and molecular structures of 5α-androstan-3β-ol-17-one and 5β-androstane-3α,l7β-diol, Acta Crystallogr. B27 (1971) 1562–1572.
[8] M.R. Silva, J.A. Paixão, M.-J.M. de Almeida, E.J.T. da Silva, M.L. Sá e, Melo, A.S.C. Neves, 3β,4α-Dihydroxy-5β-androstan-17-one, Acta Crystallogr. C52 (1996) 2892–2894.
[9] L.C.R. Andrade, M.J.B.M. de Almeida, J.A. Paixão, J.F.S. Carvalho, M.L. Sá e Melo, 3β,5α,6β-Trihydroxyandrostan-17-one, Acta Crystallogr. E67 (2011) o1056–o1057.
[10] L.C.R. Andrade, J.A. Paixão, M.J. de Almeida, E.J.T. da Silva, M.L. Sá e, Melo, A.S.C. Neves, 3α-Hydroxy-5α-androstane-4,17-dione, Acta Crystallogr. C55 (1999) 2149–2151.
[11] J.A. Paixão, L.C.R. Andrade, M.J. de Almedia, M.M.R.R. Costa, E.J.T. da Silva, M.L. Sá e Melo, A.S.C. Neves, 3α,4β-Dihydroxy-5α-androstan-17-one, Acta Crystallogr. C54 (1998) 89–91.
[12] H.N. de Armas, O.M. Peeters, N.M. Blaton, C.J. de Ranter, J.A.R. Garcia, M.R. Moreno, Y.M.A. Ginarte, 9α-Chloro-3β,11β-dihydroxy-5α-androstan-17-one, Acta Crystallog. E57 (2001) o166–o167.
[13] H.N. de Armas, O.M. Peeters, N.M. Blaton, C.J. de Ranter, J.A.R. Garcia, M.R. Moreno, Y.M.A. Ginarte, 9β,11β-Epoxy-3β-hydroxy-5α-androstan-17-one, Acta Crystallogr. E57 (2001) o39–o40.
[14] L.C.R. Andrade, J.A. Paixão, M.J.M. de Almeida, F.M.F. Roleira, M.L.M.L. Sá e Melo, A.S.C. Neves, E.J.T. da Silva, 3α,4β-Dihydroxy-5β-androstan-17-one, Acta Crystallogr. E59 (2003) o21–o23.
[15] R. Verma, D. Jasrotia, M. Bhat, Synthesis and X-ray crystallographic analysis of 17α-hydroxy-17-methylandrost-4-ene-17-one, J. Chem. Crystallogr. 36 (2006) 283–287 (Error in title: it is the 3-one and it is also a hemi hydrate).
[16] S.-J. Zhang, F. Xu, W.-X. Hu, Synthesis and crystal structure of 3β-acetoxy-5α-bromo-6β-hydroxyandrostan-17-one, J. Chem. Crystallogr. 40 (2010) 997–1001.
[17] J.I.F. Paixão, J.A.R. Salvador, J.A. Paixão, A.M. Beja, M.R. Silva, A.M.d'A.R. Gonsalves, 6β-Azido-7α-hydroxy-17-oxo-5α-androstan-3β-yl acetate, Acta Crystallogr. C60 (2004) o630–o632.
[18] C.N. Xia, B.W. Li, W.X. Hu, W. Zhou, 3β-Acetoxy-5α-chloro-6β-

hydroxyandrostan17-one, Acta Crystallogr. C63 (2007) o3107.
[19] S.-J. Zhang, F. Xu, W.-X. Hu, Synthesis and crystal structure of 3β-acetoxy-5α-bromo-6β-hydroxyandrostan-17-one, J. Chem Crystallogr. 40 (2010) 997–1001.
[20] L.C.R. Andrade, M.J.B.M. de Almeida, J.A. Paixão, J.F.S. Carvalho, M.L. e Melo, Androstane-3β,5α,6β,17β-tetrol trihydrate, Acta Crystallogr. E67 (2011) o1643–o1644.
[21] R. Verma, D. Jasrotia, A. Sawhney, M. Bhat, B.D. Gupta, Synthesis and structure determination of 3β-hydroxyandrost-5-en-17-one ($C_{19}H_{28}O_2 \cdot CH_3OH$), J. Chem. Cryst. 2004 (34) (2004) 523–528.
[22] M.M.A. Elhalim, Synthesis of new thiazolyl androstane derivatives of pharmacological interest, Bull. Fac. Pharm. Cairo Univ. 45 (2007) 227–232.
[23] M.M. Abdelhalim, E.M. Kamel, S.T. Rabie, N.R. Mohamed, Synthesis and biological evaluation of some nitrogen containing steroidal heterocycles, Steroids 76 (2011) 78–84.
[24] S. Parsons, H.D. Flack, T. Wagner, Use of intensity quotients and differences in absolute structure refinement, Acta Crystallogr. B69 (2013) 249–259.
[25] CrystalClear-SM Expert 3.1 b27 (Rigaku Oxford Diffraction, 2013).
[26] CrysAlis PRO, Agilent Technologies, Version CrysAlis PRO 1.171.39.9g: Rigaku Oxford Diffraction, 2015 (Rigaku Oxford Diffraction, 2015). http://www.rigaku.com/en/rigakuoxford.
[27] CrysAlis PRO, Agilent Technologies, Version 1.171.37.35 (release 13-08-2014 CrysAlis171 .NET) (compiled Aug 13, 2014, 18:06:01), (Rigaku Oxford Diffraction).
[28] P. McArdle, K. Gilligan, D. Cunningham, R. Dark, M. Mahon, A method for the prediction of the crystal structure of ionic organic compounds—the crystal structures of *o*-toluidinium chloride and bromide and polymorphism of bicifadine hydrochloride, CrystEngComm 6 (2004) 303–309.
[29] G.M. Sheldrick, SHELXT – integrated space-group and crystal-structure determination, Acta Crystallogr. A71 (2015) 3–8.
[30] C.B. Hübschle, G.M. Sheldrick, B. Dittrich, ShelXle a Qt graphical user interface for SHELXL, J. Appl. Cryst. 44 (2011) 1281–1284.
[31] G.M. Sheldrick, Crystal structure refinement with SHELXL7, Acta Crystallogr. C71 (2015) 3.
[32] MERCURY 3.3.9. CCDC.
[33] A.L. Spek, Structure validation in chemical crystallography, Acta Crystallogr D 65 (2009) 148.
[34] J.J. McKinnon, M.A. Spackman, A.S. Mitchell, Novel tools for visualizing and exploring intermolecular interactions in molecular crystals, Acta Crystallogr. B60 (2004) 627–668.
[35] S.K. Wolff, D.J. Grimwood, J.J. McKinnon, M.J. Turner, D. Jayatilaka, M.A. Spackman, Crystal Explorer, The University of Western Australia, 2012.
[36] D. Jayatilaka, D.J. Grimwood, Tonto: A Fortan based object-orientated system for quantum chemistry and crystallography, Comput. Sci.-ICCS 4 (2003) 142–151.
[37] J. Bernstein, R.E. Davis, L. Shimoni, N.L. Chang, Patterns in hydrogen bonding: functionality and graph set analysis in crystals, Angew. Chem. Int. Ed. Engl. 34 (1995) 1555.